J Pharmacol Sci **117**, 253 – 264 (2011)

Journal of Pharmacological Sciences

Full Paper

Identification and Role of Muscarinic Receptor Subtypes Expressed in Rat Adrenal Medullary Cells

Keita Harada[1], Hidetada Matsuoka[1], Takeyoshi Sata[2], Akira Warashina[1], and Masumi Inoue[1,*]

[1]*Department of Cell and Systems Physiology,* [2]*Department of Anesthesiology, School of Medicine, University of Occupational and Environmental Health, Kitakyushu 807-8555, Japan*

Received July 13, 2011; Accepted October 11, 2011

Abstract. The muscarinic receptor is known to be involved in the acetylcholine (ACh)-induced secretion of catecholamines in the adrenal medullary (AM) cells of various mammals. The muscarinic receptor subtype involved and its physiological role, however, have not been elucidated yet. Thus, we investigated these issues in acutely isolated rat AM cells and perfused rat adrenal medulla. The RT-PCR analysis revealed the presence of M_2, M_3, M_4, and M_5 mRNAs. Immunocytochemistry with specific antibodies showed that M_5-like immunoreactivities (IRs) were detected at half the cell membrane area, which was much larger than that with M_3- or M_4-like IRs. Muscarine produced inward currents in a dose-dependent manner. Pilocarpine, McN-A-343, and oxotremorine were less efficient than muscarine; and RS-86, which has no action on the M_5 receptor, produced no current. Electrical stimulation of nerve fibers produced a frequency-dependent increase in the Ca^{2+} signal in perfused adrenal medullae. Muscarinic receptors were found to be involved in neuronal transmission in AM cells in the presence of a cholinesterase inhibitor, which suppresses ACh degradation. We concluded that the M_5 receptor is the major muscarinic receptor subtype in rat AM cells and may be involved in neuronal transmission under conditions where ACh spills over the synapse.

Keywords: muscarinic receptor, adrenal medulla, transmission, Ca imaging, TASK channel

Introduction

Adrenal medullary (AM) cells secrete catecholamines in response to synaptic input from the splanchnic nerve. Although muscarinic acetylcholine (ACh) receptors have biochemically and/or functionally been detected in guinea-pig (1, 2), cat (3), bovine (3, 4), porcine (5), chicken (6), rat (7, 8), and human (9) chromaffin cells, their role in neurotransmission from the splanchnic nerve is controversial (1, 8, 10 – 14). Furthermore, which subtypes of muscarinic receptors are expressed in chromaffin cells has not been determined without ambiguity (3, 15, 16). We recently reported that muscarinic receptor stimulation induced inhibition of TWIK-related acid-sensitive K^+ (TASK) 1 channels, one type of leakage K^+ channels (17), with the consequent depolarization and activation of voltage-dependent Ca^{2+} channels in rat AM cells (7). Oxotremorine-M, but not oxotremorine, was efficient in this inhibition, similar to muscarine. These pharmacological properties of muscarinic receptors involved in the suppression of TASK channels raises the possibility that muscarinic receptor subtypes coupled with phospholipase C (M_1, M_3, or M_5; M_1 group) are involved rather than those coupled with adenylate cyclase (M_2 or M_4; M_2 group) (18). The first aim of the present experiment was to elucidate which muscarinic receptor subtypes are expressed in rat AM cells and then to identify the subtype involved in the inhibition of TASK channel activity. For the latter purpose, pharmacological tools were used for several reasons. First, muscarinic receptor subtypes involved in certain cellular responses are not always the same in various mammalian cells. The muscarinic receptor subtype involved in inhibition of N-type Ca^{2+} channels turned out to be of the M_4 and M_2 subtype in cervical sympathetic ganglion neurons of rats (19) and mice (20), respectively. Thus, results obtained from knockout mice may not always be the case in rats. Second, genetic ablation of a certain receptor subtype

*Corresponding author. minoue@med.uoeh-u.ac.jp
Published online in J-STAGE on November 18, 2011 (in advance)
doi: 10.1254/jphs.11125FP

may induce compensational changes in expression of other subtypes (21) and/or uncover involvement of other subtypes whose physiological significance is not apparent (22). The second aim was to clarify whether muscarinic receptors mediate neuronal transmission from the splanchnic nerve. In previous experiments (8, 10), the effects of cholinergic inhibitors on neuronal transmission were examined with the measurement of secreted catecholamines. Thus, a change in catecholamine secretion during application of the inhibitors might have been due to a time-dependent decline of secretory activity in AM cells. This possibility was minimized in the present experiment by appreciating the Ca^{2+} signal in AM cells. Although the absolute value of an electrically evoked increase in the Ca^{2+} signal in AM cells successively decreased with stimulation of the splanchnic nerve, the relatively expressed value of a change in the Ca^{2+} signal was rather constant (23). The results indicated that M_3, M_4, and M_5 muscarinic receptors are expressed at the mRNA and protein levels in rat AM cells and that the M_5 receptor may be mainly involved in the inhibition of TASK channels.

Materials and Methods

Source of agents

Muscarine chloride, oxotremorine sesquifumarate salt, and pilocarpine hydrochloride were obtained from Sigma-Aldrich (St. Louis, MO, USA); collagenase was from Yakult (Tokyo); hexamethonium chloride (C6), nicotine, and atropine sulfate were from Nacalai (Kyoto); neostigmine bromide was from Wako (Osaka); McN-A-343 (McN-A) was from RBI (Natick, MA, USA); muscarinic toxin 3 (MT3) was from Peptide Institute (Minoh); VU01844670 (VU70) and RS-86 were kindly provided by P. J. Conn (Vanderbilt University, NIH MLPCN program, Nashville, TN, USA) and Novartis (Basel, Switzerland), respectively.

Animals

Rats weighing 200 – 400 g (n = 55) were used. All experimental procedures involving animals were carried out in accordance with institutional guidelines and approved by the Institutional Animal Care and Use Committee of the University of Occupational and Environmental Health.

Whole-cell recording

The animals were killed by cervical dislocation and the adrenal glands were excised and immediately put into an ice-cold Ca^{2+}-deficient balanced salt solution in which 1.8 mM $CaCl_2$ was simply omitted from standard saline. The standard saline contained 137 mM NaCl, 5.4 mM KCl, 1.8 mM $CaCl_2$, 0.5 mM $MgCl_2$, 0.53 mM $NaHPO_4$, 5 mM D-glucose, 5 mM Hepes, and 4 mM NaOH (pH 7.4). The adrenal cortex was removed from the adrenal gland using microscissors and forceps under stereoscopic observation. The adrenal medulla was cut into two or three pieces and then incubated in a 0.5% collagenase–containing Ca^{2+}-free solution at 36°C for 30 min. The preparations were gently stirred with 100% O_2 gas for the first half of the incubation. After the incubation, the tissues were washed several times and kept in the Ca^{2+}-free solution at 5°C until cell dissociation for current recordings. One or two pieces of the tissues were put into a bath apparatus, which was placed on an inverted microscope, and the AM cells were dissociated mechanically with fine needles. Thereafter, the dissociated cells were allowed to adhere to the bottom for a few minutes before the bath apparatus was perfused with saline at a rate of 1 $ml \cdot min^{-1}$. The whole-cell current was recorded in an isolated rat AM cell using the nystatin perforated patch method, as described elsewhere (16). The current was recorded with an Axopatch 200A amplifier (Axon, Foster City, CA, USA) and then fed into a thermal recorder after low-pass filtering at 15 Hz and into a DAT recorder. The standard pipette solution contained 120 mM potassium isethionate, 20 mM KCl, 10 mM NaCl, 10 mM Hepes, and 2.6 mM KOH (pH 7.2). On the day of the experiment, nystatin dissolved in dimethyl sulfoxide (5 mg in 100 μl) was added to the pipette solution at a final concentration of 100 $\mu g \cdot ml^{-1}$ while the solution was being vortex-mixed. All of the chemicals were bath applied. The membrane potential was corrected for a liquid junction potential of −3 mV between the standard pipette solution and saline. For the analysis of the dose dependence of current responses to muscarine, the evoked current (I) was fitted by nonlinear regression analysis to a Hill equation $I = (I_{max} \times \chi) / (K_A + \chi)$, where I_{max} represents the maximum value of I, χ is the concentration of muscarine, and K_A is the concentration (EC_{50}) of muscarine responsible for half the maximum response. The experiments were carried out at 26°C ± 2°C. The data were expressed as mean ± S.E.M. and statistical significance was determined by Student's paired or unpaired *t*-test.

Immunoblot

The brain, heart, and adrenal medulla were minced and homogenized in ten volumes of a solution containing 10 mM Tris-HCl (pH 7.4), 150 mM NaCl, and a protease inhibitor cocktail [1 mM 4-(2-aminoethyl) benzene sulphonyl fluoride, 0.3 μM aprotinin, 2 μM E-64, 1 mM EDTA, 2 μM leupeptin] (Calbiochem, San Diego, CA, USA). The homogenates were centrifuged at 500 × *g* for 10 min at 4°C to remove the cell debris and then the

supernatants were mixed with equal volumes of a buffer containing 25 mM Tris-HCl (pH 6.8), 4% SDS, and 20% glycerol. Protein concentrations in the samples were determined with a BCA protein assay kit (Pierce, Rockford, IL, USA). Since catecholamine was found to interfere with the assay system, the proteins in the adrenal medulla samples were precipitated with acetone and then the precipitate dissolved in the Laemmli buffer was subjected to protein measurement. After the addition of 2-mercaptoethanol (final content, 5% v/v) and bromophenol blue (0.05% w/v) to the sample, the proteins were separated by 10% (w/v) SDS-PAGE and then transferred to a polyvinylidene difluoride (PVDF) membrane. The membrane was blocked with 5% (w/v) fat-free powdered milk dissolved in TBS-T solution, which contained 10 mM Tris-HCl (pH 7.6), 150 mM NaCl, and 0.1% Tween 20. The PVDF membrane was incubated with rabbit anti-M_1 antibody (Ab) (Frontier Institute, Ishikari) (24), rat anti-M_2 monoclonal antibody (mAb) (sc-71531; Santa Cruz Biotechnology, Santa Cruz, CA, USA), rabbit anti-M_3 Ab (AMR-006; Alomone, Jerusalem, Israel), rabbit anti-M_4 Ab (6391-2170; Biogenesis, Poole, UK), mouse anti-M_4 mAb (MAB1576; Chemicon, Temecula, CA, USA), or mouse anti-actin mAb (MAB1501R, Chemicon). The immunoreaction was detected by incubating the membrane with a respective secondary Ab linked to horseradish peroxidase (Amersham, Buckinghamshire, UK) and then with ECL-Plus (Amersham). Immunoblotting was repeated at least three times for each Ab.

Immunocytochemistry

After collagenase treatment, one or two pieces of adrenal medulla tissue were placed into a dish with non-fluorescent glass (MatTek, Ashland, MA, USA) and then dissociated using fine needles. The dissociated AM cells were fixed in 2% paraformaldehyde in phosphate-buffered saline (PBS, pH 7.2) for 1 h and then pre-incubated in PBS with 5% fetal bovine serum and 0.3% Triton-X for 30 min. For indirect immunofluorescence studies, the cells were treated with anti-M_1 Ab, anti-M_2 mAb, anti-M_3 Ab, anti-M_4 mAb, rabbit anti-M_5 Ab (6391-2190, Biogenesis), or rabbit anti-PSD-93 Ab (AB5168; Millipore, Temecula, CA, USA). After incubation, the cells were washed three times in PBS and then treated with a respective secondary Ab conjugated with Alexa 488 or 546 (Molecular Probes, Eugene, OR, USA). The fluorescence was observed using confocal laser scanning microscopy (LSM5Pascal; Carl Zeiss, Tokyo). The objective lens was an oil-immersion lens with a magnification of × 63 and a numerical aperture of 1.4. For Alexa 488, a 488-nm laser was used and 510 – 560 nm emission was observed (FITC-like fluorescence), whereas for Alexa 546, a 543-nm laser was used and emission above 560 nm was observed (rhodamine-like fluorescence). Immunocytochemical examination was repeated at least twice to confirm reproduction of the immunoreaction. The occupation rate of muscarinic receptor–like immunoreactivities (IRs) in the plasma membrane area was calculated by using NIH image software.

Cell culture and transfection

Human embryonic kidney (HEK) 293T cells were cultured in Dulbecco's modified Eagle's medium (Invitrogen, Tokyo) supplemented with 10% fetal bovine serum (Nichirei, Tokyo). The LipofectAMINE 2000 reagent (Invitrogen) was used to transfect HEK293T cells with an expression vector for hemagglutinin (HA)-tagged human M_1, M_2, M_3, M_4, or M_5 muscarinic receptor (Missouri S&T cDNA Resource Center, Rolla, MO, USA) according to the manufacturer's instructions. The transfected cells were placed onto glass coverslips coated with collagen Type I (BD Biosciences, San Jose, CA, USA) and then cultured for 24 h. The cells were fixed with 4% paraformaldehyde in PBS for 30 min at room temperature. After washing three times with PBS, the cells were incubated in PBS containing 0.1% Triton X-100 for 30 min and then with PBS containing 1% FBS for 1 h at room temperature. The cells were treated with mouse anti-HA mAb (sc-7392, Santa Cruz) or rabbit anti-HA Ab (A190-108A; Bethyl Laboratories, Montgomery, TX, USA) and anit-M_1 Ab, anti-M_2 mAb, anti-M_3 Ab (sc-9108, Santa Cruz), anti-M_4 mAb, or anti-M_5 Ab and then treated with the secondary Abs. The coverslips were mounted in 50% glycerol containing 1 $mg \cdot ml^{-1}$ 4-diaminobenzene, and immunostaining was observed with LSM5Pascal.

RT-PCR

Poly(A)$^+$RNA was isolated from rat brain and adrenal medulla using the Micro-fast track kit (Invitrogen) according to the manufacturer's instructions. In order to eliminate the genomic DNA, the extracted nucleotides were treated with DNase I of amplification grade (Invitrogen) for 15 min and then the enzyme reaction was stopped by the addition of 25 mM EDTA and by incubation at 65°C for 15 min. The Oligo dT primer was utilized for the reverse transcriptase (RT) reaction to obtain cDNAs. The PCR reactions were carried out with 0.5 μl of DNA template, 4 pmol of primers (Table 1), 2 mM of dNTPs, 0.5 units of rTaq (Takara, Otsu), and PCR buffers supplied with the kit in a final volume of 50 μl. The PCR protocol used initially started with a 2 min denaturation step at 94°C, followed by 30 to 40 cycles of the profile consisting of 30 s of denaturation at 94°C, 30 s of annealing at 54°C to 60°C, and 30 s of extension at 72°C. In each PCR reaction, the PCR product of 198 bp for

Table 1. Primer sequences used for PCR of the muscarinic receptors subtype 1 – 5 (*CHRM 1 – 5*) and *β*-actin (*ACTB*)

Target gene	Forward	Reverse	PCR product size (bp)
CHRM1	5′-acttcctgctgagcctggcc-3′	5′-tctgtctcccggtagatgcg-3′	462
CHRM2	5′-ccctctacactgtgattggc-3′	5′-agcaccatgacattgtatgg-3′	963
CHRM3	5′-acttcctcttaagcctggcc-3′	5′-tggtcttggtccatctgctc-3′	679
CHRM4	5′-acatcctggtgatgctgtcc-3′	5′-tggactcattggaagtgtcc-3′	742
CHRM5	5′-atgtcttggtcatgatctcc-3′	5′-gaggtcagccaggtccttgg-3′	548
ACTB	5′-cctgggtatggaatcctgtggcat-3′	5′-ggagcaatgatcttgatcttc-3′	198

β-actin mRNA was co-amplified and used as an internal standard. The PCR products were separated by 1.5% agarose gel electrophoresis and stained with ethidium bromide.

Perfusion experiment

The adrenal glands were removed from the rats under pentobarbital (60 mg·kg^{-1}, i.p.) anesthesia and then perfused retrogradely via the adrenal vein with saline at a rate of 0.15 ml·min^{-1} (25). The glands were subjected to a 40 min recurrent perfusion with 1 ml saline containing 10 μM Fluo-4 AM (Molecular Probes) and 0.2% Pluronic F 127 (Sigma-Aldrich), and then part of the adrenal cortex covering the medulla was carefully removed using microscissors. The adrenal gland was placed between one pair of silver circles for electrical stimulation and then the gland was transferred to a chamber with the naked medulla on the glass bottom. The chamber was mounted onto the stage of the confocal laser scanning microscope and the adrenal gland was continuously perfused at 25°C – 28°C. Illumination with 488 nm was provided by an argon laser and the emission above 510 nm was monitored. Fluorescence images were acquired every 5 s. The extent of photobleaching was estimated by a curve fitting of the intensities of responsive areas (up to 8 areas in a frame) in the resting state with a polynomial function ($at^2 + bt + c$, where a, b, and c are constants and t is time). The intensity in each area was then corrected for photobleaching. A change in fluorescence intensity in response to electrical stimulation or a cholinergic agonist was expressed as a fraction of the resting level. This relative value of change was averaged for each frame. Square pulses of 1.5-ms duration and 50 V (8) were applied to the preparation at a frequency of 0.5 to 10 Hz with a stimulator (SEN-2201; Nihon Kohden, Tokyo). The effects of hexamethonium chloride and/or atropine on the Ca^{2+} signal in response to electrical stimulation were evaluated in the preparations where transsynaptically evoked Ca^{2+} signals did not diminish by more than 20% after washing out the chemicals. The number of data represented that of adrenal glands used in the perfusion experiments.

Results

Identification of muscarinic receptor subtypes

To identify muscarinic receptor subtypes expressed in the rat adrenal medulla, PCR analysis was performed with cDNAs obtained from the rat brain and adrenal medulla. The upper panel in Fig. 1A shows that PCR in brain cDNA samples with each set of primers resulted in products with the estimated sizes, indicating that the primer sets were efficient. When cDNA samples of the adrenal medulla were subjected to PCR analysis, products for the four subtypes of muscarinic receptors (M_2 to M_5) were obtained, but not for M_1. On the other hand, PCR in RNA samples not treated with reverse transcriptase resulted in no products for any of the muscarinic receptor subtypes (data not shown), indicating that the obtained PCR products were not genomic DNA-derived amplificants. The results revealed that the M_2, M_3, M_4, and M_5 receptors are expressed at the mRNA level in the rat adrenal medulla. Next, the expression of muscarinic receptor subtypes at the protein level was examined with immunoblotting. An anti-M_1 Ab detected a major band of 63 kDa in the homogenate of rat brain, as noted in mouse brain (24), but this band was not in that of the adrenal medulla. An anti-M_2 mAb recognized bands of 50 and 70 kDa in the homogenates of rat brain and heart, but not of the adrenal medulla, whereas it slightly detected a band of 48 kDa in the latter. Since the molecular size of the M_2 receptor subtype in immunoblotting is about 70 kDa (26), it was concluded that the M_2 protein is not expressed in rat adrenal medulla. An anti-M_3 Ab recognized a 75-kDa band in the homogenate of rat brain, but not of adrenal medulla, as was noted with a different anti-M_3 Ab in our previous experiment using guinea pigs (27). For the detection of M_4 receptors, two different anti-M_4 Abs, which were monoclonal and polyclonal, were used. Both of them recognized 48-kDa bands in the rat

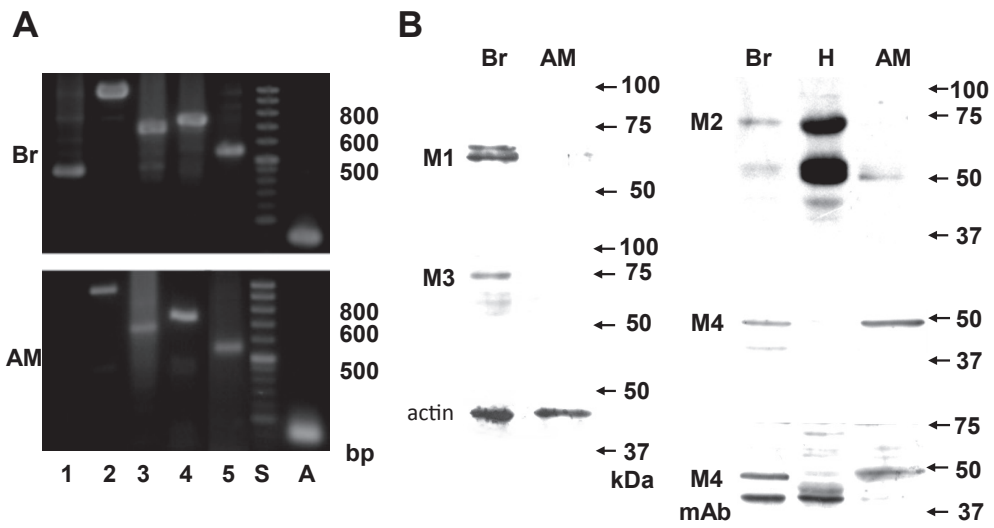

Fig. 1. Identification of muscarinic receptor subtypes expressed in the rat adrenal medulla. A: RT-PCR analysis for muscarinic receptor subtypes of cDNAs of the rat brain (Br) and adrenal medulla (AM). Electrophoresis of PCR products for five muscarinic receptor subtypes (M_1, 462 bp; M_2, 963 bp; M_3, 679 bp; M_4 742 bp; M_5, 548 bp) and β-actin (A, 198 bp). B: immunoblots for M_1, M_2, M_3, M_4, and actin. The same amounts of proteins (6 or 8 μg) in homogenates of rat Br, heart (H), and AM were loaded for each lane and probed with anti-muscarinic receptor subtype and anti-actin Abs (see Materials and Methods).

brain and adrenal medulla, but not in the heart, a value which is the same as that of recombinant M_4 proteins expressed in Chinese hamster ovary cells (28). These results strongly indicated that the M_4 protein is expressed in the rat adrenal medulla. The M_5 receptor was not studied in an immunoblot because of uncertainty of the specificity of the Ab used.

The expression of muscarinic receptor subtypes was further examined immunocytochemically. Since specificity of anti-muscarinic receptor subtype Abs in immunohistochemistry was seriously questioned (29, 30), their reliabilities in immunocytochemistry were examined in HEK293T cells where M_1, M_2, M_3, M_4, or M_5 tagged with HA was exogenously expressed. Figure 2A clearly shows that each subtype-specific Ab only stained HEK293T cells expressing HA. The detailed inspection of each staining, however, revealed that HA-like IRs were mainly confined at the cell periphery, probably the plasma membrane, whereas muscarinic receptor–like IRs were sometimes present not only at the cell periphery, but also inside the cells. The crossreactivities of the anti-M_5 and anti-M_4 Abs were explored in HEK293T cells in which HA-M_1, HA-M_3, or HA-M_4, and HA-M_5 were expressed for the former and the latter, respectively (Fig. 2B). The anti-M_5 and anti-M_4 Abs turned out to be specific for each subtype: the former did not recognize the M_1, M_3, or M_4, whereas the latter also failed to detect the M_5. The results demonstrated without ambiguity that the anti-muscarinic receptor Abs are specific for each subtype at least for immunocytochemical studies. Figure 3 shows confocal images of isolated rat AM cells immunostained with the Abs. M_1- or M_2-like IRs were not detected in 10 and 10 AM cells examined, respectively. M_3-like IRs were observed at the cell periphery in 4 of the 10 cells examined. On the other hand, M_4- and M_5-like IRs were consistently detected at the cell periphery in all the cells examined (n = 6 for M_4 and n = 7 for M_5). Figure 3B represents a summary of IRs for muscarinic receptors present at the cell periphery in AM cells. It is evident that the major subtypes present at the cell membrane were M_5 and M_4: the former and the latter were detected at about 50% and 10% of the cell periphery, respectively.

Muscarinic receptor subtypes involved in TASK channel inhibition

The pharmacological properties of muscarinic receptors involved in TASK channel inhibition were examined with the patch clamp technique. The bath application of muscarine produced an inward current at the holding potential of −50 mV (Fig. 4A) or −30 mV (Fig. 4B). The relative amplitudes of currents in response to the various concentrations of muscarine, which were expressed relative to the 30 μM muscarine–induced current in the same cells, showed a good agreement with the Hill equation with an EC_{50} of 11.2 μM and an I_{max} of 1.39. In contrast to muscarine, pilocarpine, McN-A, and oxotremorine were found to be partial agonists for the inhibition of TASK channel activity (Fig. 4: A and C): the amplitudes of inward currents evoked by 30 μM pilocarpine, McN-A, and oxotremorine were 38% ± 4% (n = 10), 34% ± 5% (n = 10), and 54% ± 8% (n = 6) of the 30 μM muscarine–induced currents in the same cells, respectively. RS-86, a muscarinic agonist which is a full agonist for the M_1 to M_4 receptors and has no potency against the M_5 receptor (31, 32), was found to be totally inefficient in inhibiting TASK channel activity (Fig. 4: B and C). Finally, the effects of VU70, which has been developed to be specific

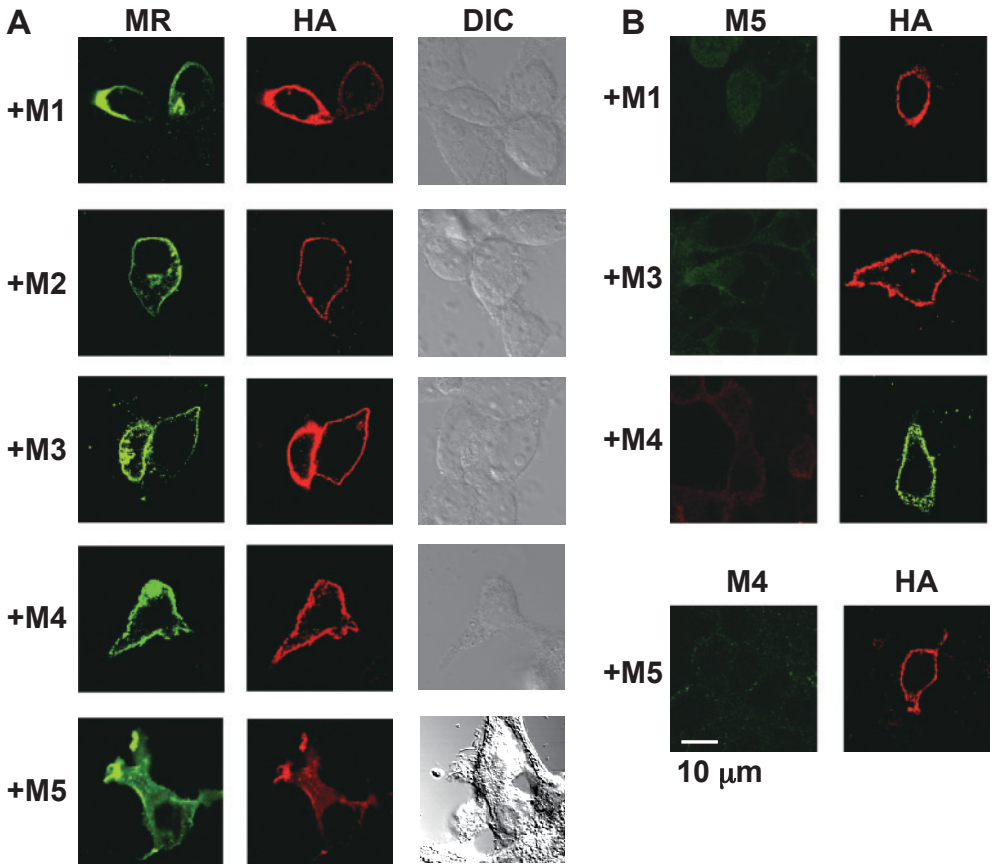

Fig. 2. Specificity of anti-muscarinic receptor subtype Abs. A: confocal images of double staining for muscarinic receptor subtype (MR: M_1, M_2, M_3, M_4, or M_5) and HA in HEK293T cells transfected with construct encoding for HA-M_1 (+M1), HA-M_2 (+M2), HA-M_3 (+M3), HA-M_4 (+M4), or HA-M_5 (+M5). DIC represents a differential interference contrast image. Note that anti-muscarinic receptor subtype Ab only labeled transfected cells. B: no cross-reactivity of anti-M_5 and anti-M_4 Abs. Expression of HA-M_1, HA-M_3, or HA-M_4 in HEK293T cells was probed with anti-M_5 Ab, whereas that of HA-M_5 was probed with anti-M_4 Ab. Green and red represent FITC- and rhodamine-like fluorescence, respectively (see Materials and Methods). The cells were treated overnight with anti-muscarinic receptor subtype Ab and anti-HA Ab. The dilution of Abs was 1:50 for M_1 to M_4, 1:100 for M_5, and 1:100 for HA.

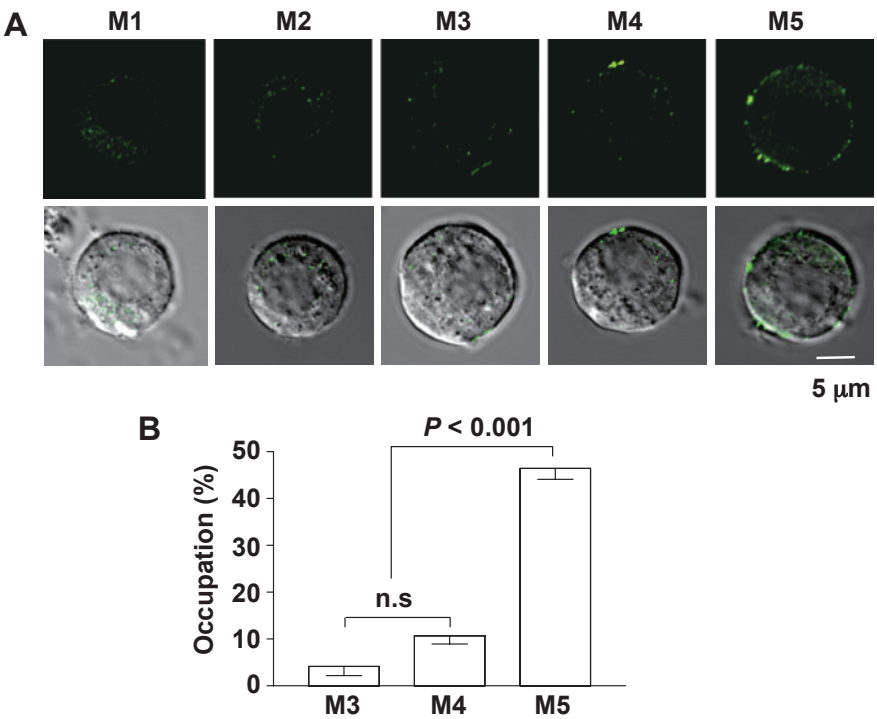

Fig. 3. Immunocytochemistry for muscarinic receptor subtypes in isolated rat adrenal medullary cells. A: staining for muscarinic receptor subtypes (M_1, M_2, M_3, M_4, and M_5) in dissociated adrenal medullary (AM) cells. Fluorescence image (upper) and overly image of fluorescence image on DIC image (lower) were shown for each subtype. B: summary of immunoreactivities for M_3, M_4, and M_5. The membrane area with immunoreactivities was expressed as a fraction of the cell perimeter. The data represent mean ± S.E.M. (M_3, n = 10; M_4, n = 6; M_5, n = 7).

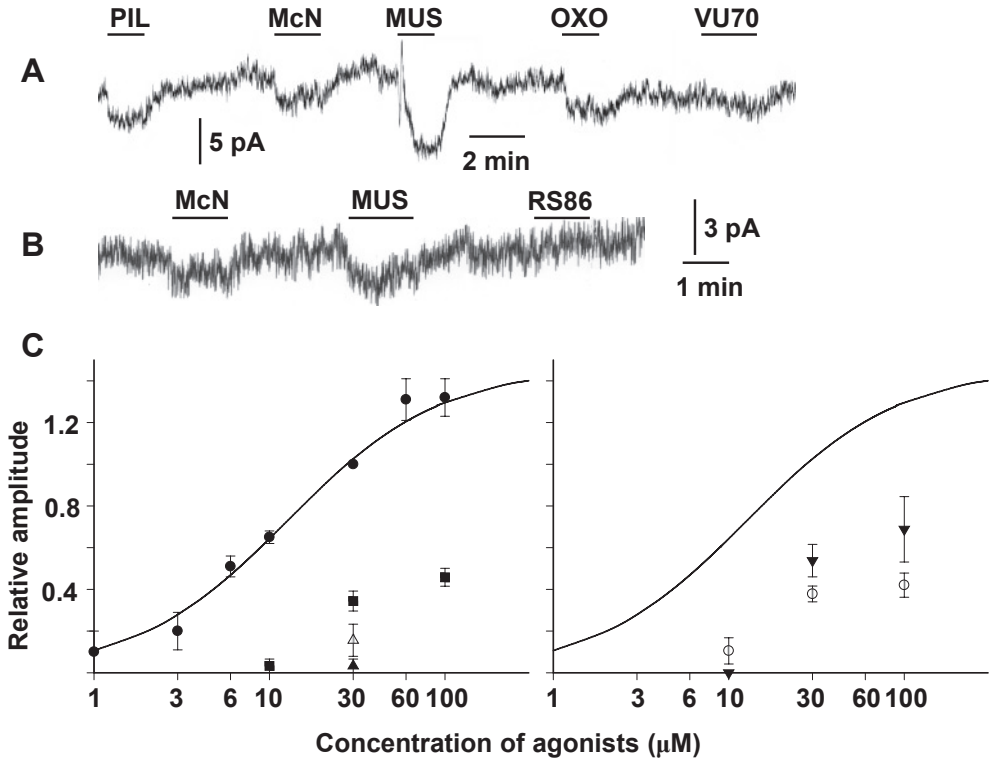

Fig. 4. Different efficacies of muscarinic agonists in producing inward currents in rat AM cells. A and B: traces of whole-cell currents in response to pilocarpine (PIL), McN-A (McN), muscarine (MUS), oxotremorine (OXO), and VU70 and to McN, MUS, and RS86 in two different dissociated AM cells, respectively. The concentration of each muscarinic agonist was 30 μM. Whole-cell currents were recorded at −50 mV (A) and −30 mV (B) with the nystatin method. C: summary of dose dependence of MUS (closed circle), McN (closed square), RS86 (closed triangle), VU70 (open triangle), OXO (inverted closed triangle), and PIL (open circle)-induced inward currents. Mean ± S.E.M. are plotted against concentrations of agonists (MUS, n = 5 – 13 for each point; McN, n = 4 – 10; OXO, n = 2 – 6; PIL, n = 4 – 10; VU70, n = 5; RS86, n = 7). The amplitude of agonist-induced current was expressed as a fraction of the 30 μM muscarine–induced current in the same cells. The line represents a Hill equation: I_{max} = 1.39 μM and EC_{50} = 11.2 μM.

for M_1 (33), were examined. Figure 4, A and C, shows that 30 μM VU70 induced marginal inward currents in five AM cells: the VU70-induced inward currents were 16% ± 8% (n = 5) of the 30 μM muscarine–induced currents in the same cells. All of the agents used, except for muscarine and VU70, are full agonists for M_4 and have a partial or no agonistic action for M_5. These pharmacological studies may negate the involvement of M_4 in the muscarine-induced current. This notion was further examined with MT3. This peptide inhibitor, which is specific to M_4 (18, 34, 35), had no action on the current response to muscarine: 10 and 30 μM muscarine–induced currents in the presence of 0.1 μM MT3 were 86.7% ± 6.6% (n = 3) and 92.4% ± 3.5% (n = 6) of those in its absence, respectively.

Perfusion experiment

Whether muscarinic receptors were involved in synaptic transmission in AM cells or not was examined in rat adrenal medulla that was retrogradely perfused through the adrenal vein and loaded with the Ca^{2+} indicator Fluo-4. The transmural stimulation of the adrenal gland with a 1.5-ms pulse of 50 V for 30 s resulted in trans-synaptic activation of AM cells with an increase in the Ca^{2+} signal in a frequency-dependent manner. The relative amplitudes of such increases in response to electrical stimulation, which were expressed as a fraction of the resting level were 0.246 ± 0.019 (n = 16), 0.316 ± 0.019 (n = 24), 0.563 ± 0.037 (n = 19), and 0.641 ± 0.060 (n = 11) at the frequency of 0.5, 1, 5, and 10 Hz, respectively. Retrograde application of 30 μM nicotine produced a Ca^{2+} signal that increased to a peak and then declined towards a plateau level, as was noted with the current response to nicotine under the voltage clamp conditions (36). Electrical stimulation performed during the nicotine-induced Ca^{2+} signal resulted in little, if any, further increase in the Ca^{2+} signal, as shown in Fig. 5A. When a similar experiment was performed during application of 30 μM musca-

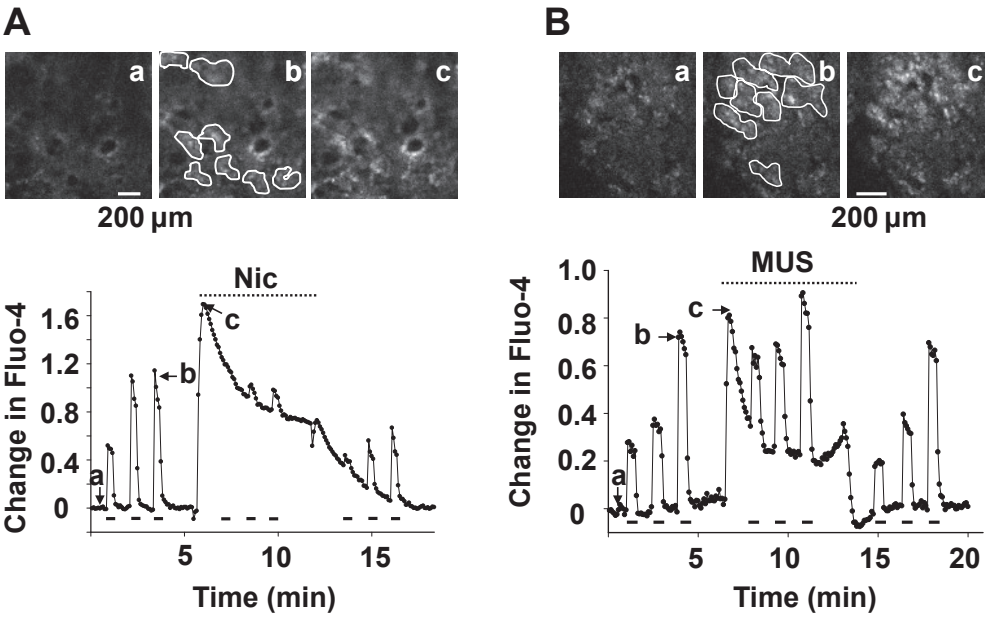

Fig. 5. Effects of electrical field stimulation on intracellular Ca^{2+} concentration ($[Ca^{2+}]_i$) in fluo-4–loaded AM cells. Upper panel in A and B: confocal images of fluo-4 fluorescence in rat adrenal medulla. Lower panel in A and B: relative values of change in fluorescence intensity plotted against time. The adrenal gland was retrogradely perfused through the adrenal vein with saline. Nerve fibers remaining in the gland were electrically stimulated with 60-V pulses of 1.5-ms duration at 1, 10, and 20 Hz (A) and 0.5, 1, and 5 Hz (B) during the indicated periods (bars). Nicotine (Nic) and muscarine (MUS), each at 30 μM, were added to the perfusion solution during the indicated period (interrupted lines). Fluorescence intensities in the areas indicated in b were measured. After correction for the decline due to photobleaching, the increase in fluorescence intensity in response to electrical stimulation and nicotine or muscarine was expressed as a fraction of the resting level (see Materials and Methods). a, b, and c in the upper panels correspond to a, b, and c in the lower panels.

rine, an increase in the Ca^{2+} signal in response to electrical stimulation was not markedly affected: increases in the Ca^{2+} signal electrically evoked at the frequency of 0.5, 1, and 5 Hz in the presence of muscarine were 90.3% ± 6.1% (n = 3), 84.3% ± 7.8% (n = 6), and 78% ± 6.1% (n = 5) of the corresponding increase in its absence, respectively (Fig. 5B). The value obtained at 0.5 and 1 Hz in the presence of muscarine was not significantly different from the control in the absence, suggesting that muscarinic receptor stimulation did not affect voltage-dependent Ca^{2+} channel activity in rat AM cells. The different effects of nicotine and muscarine on Ca^{2+} responses evoked by electrical stimulation raise the possibility that the marked suppression of the electrically evoked response during nicotine application may have been due to occlusion of nicotinic ACh receptors and the muscarinic receptor may not be involved in synaptic transmission under the present experimental conditions.

This possibility was examined by the application of the nicotinic receptor antagonist C6 and/or the muscarinic receptor antagonist atropine. Figure 6A shows that increases in the Ca^{2+} signal in response to electrical stimulation diminished by about 90% in the presence of 500 μM C6, irrespective of its frequency, and that the remaining component was not affected by the further addition of 3 μM atropine. The Ca^{2+} response to electrical stimulation was restored to the control level after washing out the antagonists. On the other hand, the application of 3 μM atropine alone did not suppress the increase in the Ca^{2+} signal in response to electrical stimulation: peak amplitudes of the Ca^{2+} signal increases electrically evoked at 1, 5 and 10 Hz in the presence of atropine were 95.3% ± 2.4% (n = 6), 94.8% ± 2.8% (n = 6), and 95.5% ± 2.4% (n = 6) of those in the absence. These results clearly indicated that muscarinic receptors are not involved in synaptic transmission in the order of milliseconds to seconds in AM cells under normal conditions. It is likely that muscarinic receptors are located in the extrasynaptic membrane in AM cells. This possibility was examined by application of the cholinesterase inhibitor neostigmine, which may increase the extent to which ACh spills out over the synapse (37), that is, the content of ACh diffusing to the extrasynaptic site should increase because of suppression of the degradation of ACh. The application of 10 μM neostigmine enhanced the peak of the Ca^{2+} signal in response to electrical stimulation, irrespective of the frequency (1 Hz: 133% ± 13% increase, n = 8; 5 Hz: 122% ± 8%, n = 7; 10 Hz: 122% ± 8%,

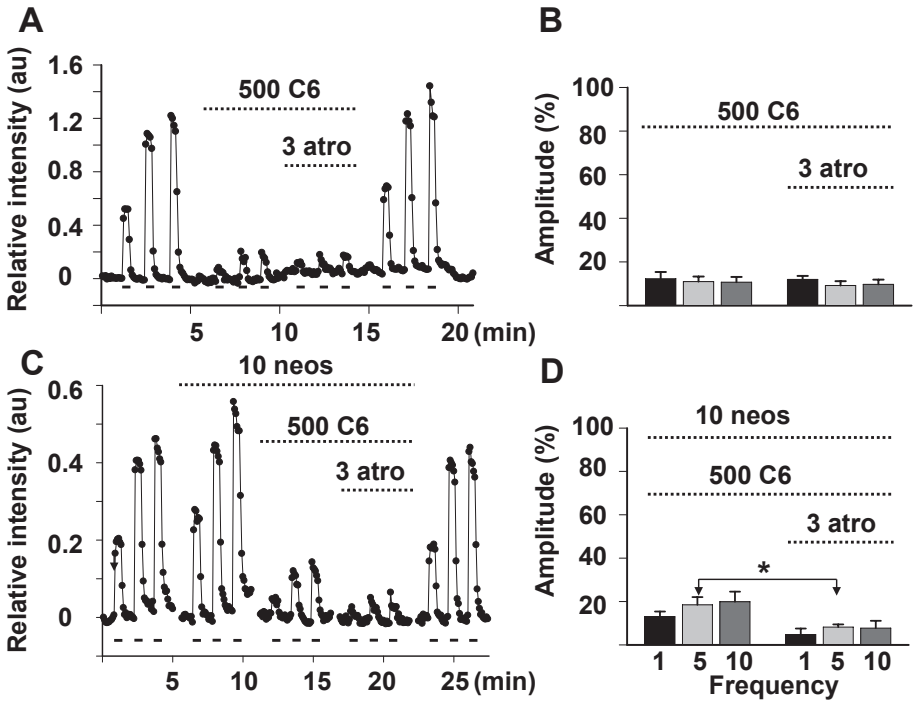

Fig. 6. Effects of C6 and atropine on increase in $[Ca^{2+}]_i$ in AM cells in response to electrical field stimulation in the presence and absence of neostigmine. A and C: relative values of change in the Ca^{2+} signal in response to electrical stimulation in the presence and absence of chemicals plotted against time. A Ca^{2+} signal in the rat adrenal medulla was observed and a change in the Ca^{2+} signal was expressed, as explained in the figure legend for Fig. 5. Chemicals [500 μM C6, 3 μM atropine (atro), and 10 μM neostigmine (neos)] were added to the perfusion solution during the indicated periods (interrupted lines). Nerve fibers in the gland were electrically stimulated with 60-V pulses of 1.5-ms duration at 1, 5, and 10 Hz for 30 s during the indicated periods (bars). Fluorescence recording restarted 5 min after exchange of perfusion solution to ensure that the chemicals were sufficiently applied or washed out. B and D: summary of effects of C6 and atropine on Ca^{2+} signals evoked by electrical stimulation at 1, 5, and 10 Hz in the absence and presence of neostigmine, respectively. Relative values of change in the Ca^{2+} signal in response to electrical stimulation in the presence of cholinergic inhibitors were expressed as fractions of those before applications of the inhibitors. The asterisk represents statistical significance ($P < 0.05$). The data represent mean ± S.E.M. of n = 5 (B) and n = 4 (D).

n = 7) and retarded the decay of the Ca^{2+} signal following cessation of electrical stimulation (Fig. 6C). In the presence of neostigmine, the C6-insensitive component of the Ca^{2+} signals turned out to be about 20% of the maximum amplitudes, a value which was significantly larger than those in the absence of neostigmine. These remaining components were significantly reduced by the further addition of 3 μM atropine. These results clearly indicated that muscarinic receptors are involved in synaptic transmission under conditions in which ACh degradation is impaired.

Presence of M_5 at the extrasynaptic site in AM cells

The foregoing results suggested that the M_5 receptor is involved in TASK channel inhibition and that it is mainly located at the extrasynaptic site. This notion was immunocytochemically examined in isolated AM cells. PSD93-like immunoreactive materials, a protein which is a major scaffolding protein at the postsynaptic membrane in sympathetic ganglion cells (38), were detected in about 20% of the surface membrane, whereas M_5-like IRs were found in about 50% of that (Fig. 7). These immunocytochemical stainings clearly indicated that the majority of M_5 receptors are present at extrasynaptic sites.

Discussion

Muscarinic receptor subtypes involved in TASK channel inhibition

The muscarinic receptor subtypes are divided into two groups. The M_1 and the M_2 group are associated with phospholipase C activation and adenylate cyclase inhibition, respectively (18). Oxotremorine is a partial and a full agonist for the M_1 and the M_2 group (32, 39, 40), respectively, whereas muscarine and oxotremorine-M are full agonists for both (32, 40). The present experiment extended the list of partial agonists for the musca-

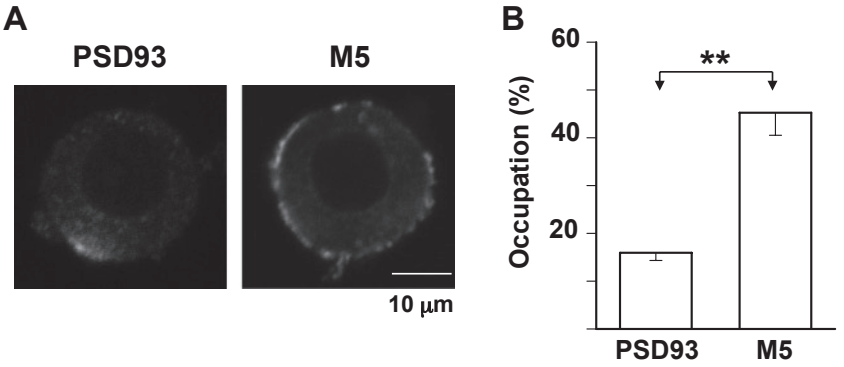

Fig. 7. Immunocytochemistry for PSD93 and M_5 receptor in rat AM cells. A: confocal images of immunostaining for PSD93 and M_5 in rat AM cells. The immunostaining for PSD93 and M_5 was performed in AM cells dissociated at the same days. B: summary of occupation rates of PSD93- and M_5-like immunoreactive materials in the cell membrane. The asterisks indicate statistical significance ($P < 0.001$). The data represent mean ± S.E.M. (PSD93, n = 4; M_5, n = 4).

rinic receptor–mediated inhibition of TASK channel activity in rat AM cells. Pilocarpine and McN-A were not efficient in producing an inward current through TASK channel inhibition, as was noted with oxotremorine (7): the amplitudes of inward currents in response to both of them were less than half the muscarine-induced currents. Pilocarpine was a partial agonist for the M_2, M_3, and M_5 receptors and a full agonist for the M_4 receptor (32, 40), whereas McN-A was a partial and a full agonist for the M_5 and the M_4 receptor, respectively (32), and had practically no action on the M_3-mediated increase in phosphatidyl inositol turnover in cell lines (32). Furthermore, VU70, a M_1 specific agonist, produced marginal inward currents, the amplitudes of which were about 10% of those in response to muscarine. These differences in efficacy of producing inward currents among the muscarinic agonists suggest the involvement of M_5 receptor rather than other subtypes, such as M_4. This notion was supported by the failure of RS-86 to induce an inward current. It was reported that RS-86 has no affinity against the M_5 and is a partial or full agonist for the remaining four muscarinic receptor subtypes (31, 32). The analysis of the effect of a muscarinic antagonist also clearly negate the involvement of M_4. The specific peptide inhibitor MT3 at 0.1 μM hardly suppressed 10 and 30 μM muscarine–induced currents, whereas it has been shown to markedly abrogate 5 μM muscarine–induced inhibition of depolarization-activated Ca^{2+} currents in rat intracardiac neurons (34).

The involvement of M_5 is consistent with biochemical and morphological findings in rat adrenal medullae. The RT-PCR analysis revealed expression of the four muscarinic subtypes, except for M_1, in the rat adrenal medulla at the mRNA level. In contrast, M_2 and M_3 proteins were not detected in the rat adrenal medulla by using immunoblotting. Two different anti-M_4 Abs recognized a 48-kDa protein and M_4-like immunoreactive materials were consistently found at the cell periphery in rat AM cells. M_5-like IRs detected with a specific Ab were present at about 50% of the cell periphery in rat AM cells, a value that was much larger than those noted for M_3- and M_4-like IRs. Although the involvement of M_5 receptor could not be directly examined because of the lack of specific M_5 agents, the pharmacological and immunocytochemical findings would sufficiently indicate that the M_5 receptor is the major subtype expressed in rat AM cells and may be involved in the muscarine-induced depolarization in rat AM cells. This notion is consistent with the participation of $G_{q/11}$-type G proteins in the receptor-mediated inhibition of TASK channel activity (41).

Role of the muscarinic receptor in neural transmissio

The present experiments extended the previous findings that the trans-synaptically evoked catecholamine release was not suppressed by atropine in perfused rat adrenal glands (8) and demonstrated that neuronal transmission in rat AM cells was partly suppressed by atropine only under conditions where ACh degradation was impaired by neostigmine. Retrograde application of 3 μM atropine in the presence of 500 μM C6 produced a further suppression of the trans-synaptically evoked increase in the Ca^{2+} signal in the absence of ACh degradation. This inhibition might have been ascribed to be a nonspecific effect of atropine, as was noted for the inhibition of nicotinic ACh receptors in guinea-pig AM cells (36). However, this possibility may be unlikely because application of 3 μM atropine alone did not produce a noticeable effect on the increase of Ca^{2+} signal in the absence of neostigmine. The finding that atropine suppressed a C6-insensitive component of the trans-synaptically evoked Ca^{2+} signal suggests the notion that the muscarinic receptors involved are located at the extrasynaptic site in rat AM cells. This idea was supported by the immunocytochemical findings. The membrane area with M_5-like IR, which was about half of the cell perimeter in one cell section, was much larger than that (about 20%) with PSD93-like IR, which may represent the postsynaptic membrane in the peripheral nervous system (38). The latter approximates the ratio of the diameter of presynaptic buttons to that of rat AM cells, which have one to four

presynaptic buttons (42).

The distribution of M_5 receptors in the body appears to be very limited: significant amounts of M_5 proteins were not detected in peripheral tissues, such as the ileum, lung, and submaxillary gland (43), whereas selected areas in the rat brain, such as dopamine neurons in the midbrain, were found to be positive for M_5 mRNA (44, 45). The M_5 receptor in the rat and mouse midbrain ventral segmental areas appears to play an important role in transmission of the neuronal information from the laterodorsal tegmentum in the pons to the nucleus accumbens. The prolonged dopamine release in the nucleus accumbens that occurred 30 – 60 min after 1-min electrical stimulation by train pulses in the rat laterodorsal tegmentum was suppressed by local administration of scopolamine, a muscarinic antagonist, into the ventral tegmental area (46) or by genetic ablation of the M_5 receptor in mice (47), whereas the dopamine release time locked to the electrical stimulation was markedly suppressed by the local application of an ionotropic glutamate receptor blocker or a nicotinic ACh receptor blocker (46). The activation of muscarinic receptors in the dopaminergic neurons in the substantia nigra and ventral tegmental area was found to induce depolarization (48), possibly through the opening of nonselective cation channels (49). These in vivo and in vitro experiments suggest that muscarinic receptors, probably M_5, are involved in an extremely slow excitatory transmission in the order of a few tens of minutes from the pons laterodorsal tegmentum to the midbrain dopaminergic neurons. Therefore, the present findings that muscarinic receptors were involved in a trans-synaptically evoked increase in excitation in the AM cells only in the presence of neostigmine may not negate the physiological significance of M_5 receptors in AM cells. Muscarinic receptors in AM cells might be involved in adrenaline secretion in response to severe stressors, such as hypoglycemia (50). A further study with knockout mice of muscarinic receptors (51) will be required to elucidate their physiological functions in AM cells.

Acknowledgments

This work was supported in part by MEXT KAKENHI (21026029 to MI) and JSPS KAKENHI (21500360 to MI and 22790222 to HM). We would like to thank P. J. Conn (Vanderbilt University, the NIH MLPCN program) and Novartis for providing VU01844670 and RS-86, respectively. We are grateful to T. Hatama for technical assistance.

References

1 Holman ME, Tonta MA, Coleman HA, Parkington HC. Muscarinic receptor activation in guinea-pig chromaffin cells causes decreased membrane conductance and depolarization. J Auton Nerv Syst. 1998;68:140–144.
2 Inoue M, Kuriyama H. Muscarinic receptor is coupled with a cation channel through a GTP-binding protein in guinea-pig chromaffin cells. J Physiol. 1991;436:511–529.
3 Ballesta JJ, Borges R, García AG, Hidalgo MJ. Secretory and radioligand binding studies on muscarinic receptors in bovine and feline chromaffin cells. J Physiol. 1989;418:411–426.
4 Eberhard DA, Holz RW. Cholinergic stimulation of inositol phosphate formation in bovine adrenal chromaffin cells: distinct nicotinic and muscarinic mechanisms. J Neurochem. 1987;49:1634–1643.
5 Forsberg EJ, Li Q, Xu Y. Cation channel activated by muscarinic agonists on porcine adrenal chromaffin cells. Am J Physiol. 1995;269:E43–E52.
6 Knight DE, Baker PF. Observations on the muscarinic activation of catecholamine secretion in the chicken adrenal. Neuroscience. 1986;19:357–366.
7 Inoue M, Harada K, Matsuoka H, Sata T, Warashina A. Inhibition of TASK1-like channels by muscarinic receptor stimulation in rat adrenal medullary cells. J Neurochem. 2008;106:1804–1814.
8 Nagayama T, Matsumoto T, Kuwakubo F, Fukushima Y, Yoshida M, Suzuki-Kusaba M, et al. Role of calcium channels in catecholamine secretion in the rat adrenal gland. J Physiol. 1999;520:503–512.
9 Pérez-Alvarez A, Albillos A. Key role of the nicotinic receptor in neurotransmitter exocytosis in human chromaffin cells. J Neruochem. 2007;103:2281–2290.
10 Alamo L, Garcìa AG, Borges R. Electrically-evoked catecholamine release from cat adrenals. Role of cholinergic receptors. Biochem Pharmacol. 1991;42:973–978.
11 Kayaalp SO, McIsaac RJ. Muscarinic component of splanchnic-adrenal transmission in the dog. Br J Pharmacol. 1969;36:286–293.
12 Olivos L, Artalejo AR. Muscarinic excitation-secretion coupling in chromaffin cells. Acta Physiol (Oxf). 2008;192:213–220.
13 Pelto-Huikko M, Dagerlind A, Kononen J, Lundberg JM, Villar M, Koistinaho J, et al. Neuronal regulation of c-fos, c-jun, and junB immediate-early genes in rat adrenal medulla. J Neurosci. 1995;15:1854–1868.
14 Wakade AR, Wakade TD. Contribution of nicotinic and muscarinic receptors in the secretion of catecholamines evoked by endogenous and exogenous acetylcholine. Neuroscience. 1983;10:973–978.
15 Fernando JC, Abdallah EA, Evinger M, Forray C, el-Fakahany EE. The presence of an M4 subtype muscarinic receptor in the bovine adrenal medulla revealed by mRNA and receptor binding analyses. Eur J Pharmacol. 1991;207:297–303.
16 Inoue M, Imanaga I. Mechanism of activation of nonselective cation channels by putative M4 muscarinic receptor in guinea-pig chromaffin cells. Br J Pharmacol. 1995;114:419–427.
17 Bayliss DA, Sirois JE, Talley EM. The TASK family: two-pore domain background K^+ channels. Mol Interv. 2003;3:205–219.
18 Caulfield MP, Birdsall NJ. International Union of Pharmacology. XVII. Classification of muscarinic acetylcholine receptors. Pharmacol Rev. 1998;50:279–290.
19 Fernandez-Fernandez JM, Wanaverbecq N, Halley P, Caulfield MP, Brown DA. Selective activation of heterologously expressed G protein-gated K^+ channels by M_2 muscarinic receptors in rat sympathetic neurones. J Physiol. 1999;515:631–637.
20 Shapiro MS, Loose MD, Hamilton SE, Nathanson NM, Gomeza

J, Wess J, et al. Assignment of muscarinic receptor subtypes mediating G-protein modulation of Ca^{2+} channels by using knockout mice. Proc Natl Acad Sci U S A. 1999;96:10899–10904.

21 Ito Y, Oyunzul L, Seki M, Fujino (Oki) T, Matsui M, Yamada S. Quantitative analysis of the loss of muscarinic receptors in various peripheral tissues in M_1-M_5 receptor single knockout mice. Br J Pharmacol. 2009;156:1147–1153.

22 Kitazawa T, Asakawa K, Nakamura T, Teraoka H, Unno T, Komori S, et al. M3 muscarinic receptors mediate positive inotropic responses in mouse atria: a study with muscarinic receptor knockout mice. J Pharmacol Exp Ther. 2009;330:487–493.

23 Matsuoka H, Harada K, Endo Y, Warashina A, Doi Y, Nakamura J, et al. Molecular mechanisms supporting a paracrine role of GABA in rat adrenal medullary cells. J Physiol. 2008;586: 4825–4842.

24 Narushima M, Uchigashima M, Fukaya M, Matsui M, Manabe T, Hashimoto K, et al. Tonic enhancement of endocannabinoid-mediated retrograde suppression of inhibition by cholinergic interneuron activity in the striatum. J Neurosci. 2007;27:496–506.

25 Warashina A, Satoh Y. Modes of secretagogue-induced $[Ca^{2+}]_i$ responses in individual chromaffin cells of the perfused rat adrenal medulla. Cell Calcium. 2001;30:395–401.

26 Luetje CW, Brumwell C, Norman MG, Peterson GL, Schimerlik MI, Nathanson NM. Isolation and characterization of monoclonal antibodies specific for the cardiac muscarinic acetylcholine receptor. Biochemistry. 1987;26:6892–6896.

27 Endo Y, Harada K, Fujishiro N, Imanaga I, Ogawa K, Inoue M. Localization of muscarinic receptor and cation channel in guinea-pig adrenal chromaffin cells. Acta Histochem Cytochem. 2005; 38:273–282.

28 Hersch SM, Gutekunst CA, Rees HD, Heilman CJ, Levey AI. Distribution of m1-m4 muscarinic receptor proteins in the rat striatum: light and electron microscopic immunocytochemistry using subtype-specific antibodies. J Neurosci. 1994;14:3351–3363.

29 Jositsch G, Papadakis T, Haberberger RV, Wolff M, Wess J, Kummer W. Suitability of muscarinic acetylcholine receptor antibodies for immunohistochemistry evaluated on tissue sections of receptor gene-deficient mice. Naunyn Schmiedebergs Arch Pharmacol. 2009;379:389–395.

30 Pradidarcheep W, Stallen J, Labruyère WT, Dabhoiwala NF, Michel MC, Lamers WH. Lack of specificity of commercially available antisera against muscarinergic and adrenergic receptors. Naunyn Schmiedebergs Arch Pharmacol. 2009;379: 397–402.

31 Hargreaves RJ, McKnight AT, Scholey K, Newberry NR, Street LJ, Hutson PH, et al. L-689,660, a novel cholinomimetic with functional selectivity for M1 and M3 muscarinic receptors. Br J Pharmacol. 1992;107:494–501.

32 Richards MH, van Giersbergen PL. Human muscarinic receptors expressed in A9L and CHO cells: activation by full and partial agonists. Br J Pharmacol. 1995;114:1241–1249.

33 Lebois EP, Bridges TM, Lewis LM, Dawson ES, Kane AS, Xiang Z, et al. Discovery and characterization of novel subtype-selective allosteric agonist for the Investigation of M1 receptor function in the central nervous system. ACS Chem Neurosci. 2010;1: 104–121.

34 Cuevas J, Adams DJ. M_4 muscarinic receptor activation modulates calcium channel currents in rat intracardiac neurons. J Neurophysiol. 1997;16:1903–1912.

35 Olianas MC, Ingianni A, Maullu C, Adem A, Karlsson E, Onali P. Selectivity profile of muscarinic toxin 3 in functional assays of cloned and native receptors. J Pharmacol Exp Ther. 1999; 288:164–170.

36 Inoue M, Kuriyama H. Properties of the nicotinic-receptor-activated current in adrenal chromaffin cells of the guinea-pig. Pflugers Arch. 1991;419:13–20.

37 Bramich NJ, Brock JA, Hirst GD. Potentiation by neostigmine of responses to vagal nerve stimulation in the sinus venosus of the toad. Auton Neurosci. 2000;82:109–114.

38 Parker MJ, Zhao S, Bredt DS, Sanes JR, Feng G. PSD93 regulates synaptic stability at neuronal cholinergic synapses. J Neurosci. 2004;14:378–388.

39 Ehlert FJ. The relationship between muscarinic receptor occupancy and adenylate cyclase inhibition in the rabbit myocardium. Mol Pharmacol. 1985;28:410–421.

40 Mistry R, Dowling MR, Challiss RA. An investigation of whether agonist-selective receptor conformations occur with respect to M_2 and M_4 muscarinic acetylcholine receptor signalling via $G_{i/o}$ and G_s proteins. Br J Pharmacol. 2005;144:566–575.

41 Chen X, Talley EM, Patel N, Gomis A, Mclntire WE, Dong B, et al. Inhibition of a background potassium channel by Gq protein α-subunits. Proc Natl Acad Sci U S A. 2006;103:3422–3427.

42 Kajiwara S, Sand O, Kidokoro Y, Barish ME, Iijima T. Functional organization of chromaffin cells and cholinergic synaptic transmission in rat adrenal medulla. Jpn J Physiol. 1997;47:449–464.

43 Dörje F, Levey A, Brann MR. Immunological detection of muscarinic receptor subtype proteins (m1-m5) in rabbit peripheral tissues. Mol Pharmacol. 1991;40:459–462.

44 Levey AI, Kitt CA, Simonds WF, Price DL, Brann MR. Identification and localization of muscarinic acetylcholine receptor proteins in brain with subtype-specific antibodies. J Neurosci. 1991; 11:3218–3226.

45 Weiner DM, Levey AI, Brann MR. Expression of muscarinic acetylcholine and dopamine receptor mRNAs in rat basal ganglia. Proc Natl Acad Sci U S A. 1990;87:7050–7054.

46 Forster G, Blaha CD. Laterodorsal tegmental stimulation elicits dopamine efflux in the rat nucleus accumbens by activation of acetylcholine and glutamate receptors in the ventral tegmental area. Eur J Neurosci. 2000;12:3596–3604.

47 Forster GL, Yeomans JS, Takeuchi J, Blaha CD. M5 muscarinic receptors are required for prolonged accumbal dopamine release after electrical stimulation of the pons in mice. J Neurosci. 2002;22:RC190.

48 Lacey MG, Calabresi P, North RA. Muscarine depolarizes rat substantia nigra zona compacta and ventral tegmental neurons in vitro through M_1-like receptors. J Pharmacol Exp Ther. 1990; 253:395–400.

49 Tozzi A, Bengtson CP, Longone P, Carignani C, Fusco FR, Bernardi G, et al. Involvement of transient receptor potential-like channels in responses to mGluR-I activation in midbrain dopamine neurons. Eur J Neurosci. 2003;18:2133–2145.

50 Cryer PE. Physiology and pathophysiology of the human sympathoadrenal neuroendocrine system. N Engl J Med. 1980; 303:436–444.

51 Matsui M, Yamada S, Oki T, Manabe T, Taketo MM, Ehlert FJ. Functional analysis of muscarinic acetylcholine receptors using knockout mice. Life Sci. 2004;75:2971–2981.